# AN OPEN-SOURCE FRAMEWORK FOR EVALUATING COOPERATIVE PERCEPTION IN URBAN AREAS

**Mario Ilic***
Chair of Traffic Engineering and Control
Technical University of Munich
Arcisstr. 21, 80333 Munich, Germany
mario.ilic@tum.de
https://orcid.org/0000-0003-2457-698X

**Mathias Pechinger**
Chair of Traffic Engineering and Control
Technical University of Munich (TUM)
mathias.pechinger@tum.de
https://orcid.org/0000-0003-2371-9870

**Tanja Niels**
Chair of Traffic Engineering and Control
Technical University of Munich (TUM)
tanja.niels@tum.de
https://orcid.org/0000-0002-8530-0285

**Evald Nexhipi**
Chair of Traffic Engineering and Control
Technical University of Munich (TUM)
evald.nexhipi@tum.de
https://orcid.org/0009-0009-6781-1581

**Klaus Bogenberger**
Chair of Traffic Engineering and Control
Technical University of Munich
https://orcid.org/0000-0003-3868-9571

* Corresponding Author

Word Count: 6630 words + 2 table(s) $\times$ 250 = 7130 words

Submission Date: August 1, 2024

**ABSTRACT**

This paper presents an open-source simulation framework for evaluating static and dynamic occlusions in urban environments, focusing on the challenges faced by Connected and Automated Vehicles (CAVs). It utilizes SUMO for traffic simulation and Python for ray tracing, enabling detailed analyses of occlusion effects without the need for complex co-simulation frameworks. Additionally, the framework introduces the observer vehicle type Floating Bike Observer (FBO), accounting for the increasing diversity of sensor-equipped vehicles in urban environments and enabling the investigation of further concepts for cooperative perception of CAVs in urban scenarios. A case study aimed at providing insights for the accurate calibration of the recently introduced Level of Visibility (LoV) metric by exploring further infrastructural and traffic-related influencing factors. The results reveal a strong sensitivity of the LoV metric towards traffic volumes and observer speed. Based on these findings, methodological adaptions of the LoV metric are proposed and discussed, such as a demand-dependent adjustment of the LoV scale and the inclusion of further influencing factors into the ray tracing method and subsequent assessment of visibility scores. Future work will deal with the optimization of the existing framework and the implementation of further applications. Furthermore, the calibration of the LoV metric will be further investigated by considering additional relevant infrastructural and traffic-related influencing factors.

*Keywords*: Floating Car Observer, Floating Bike Observer, Cooperative Perception, Level of Visibility, Open-Source Framework

## INTRODUCTION

Connected and Automated Vehicles (CAVs) have earned substantial research attention over the past decade, predominantly focusing on their deployment and performance in highway scenarios. The controlled nature of highways, characterized by predictable vehicular behavior and structured environments, has provided an ideal testing ground for developing CAV technologies. (*1*) However, the translation of these advancements to urban environments presents a unique set of challenges that increase the complexity of the operational design domain and demand further research (*2*). A substantial prerequisite for public acceptance and the deployment of CAVs in urban areas is the safe operation and continuous avoidance of accidents involving CAVs and other road users (*3*).

Urban scenarios are inherently more complex than highway scenarios due to several factors. Firstly, the intricate layout of urban intersections and the dense, chaotic nature of city traffic contribute to a significantly more challenging environment for CAVs. Unlike highways, urban areas are teeming with static and dynamic occlusions caused by buildings, parked vehicles, and other physical barriers. (*4*) These occlusions obstruct the CAVs' field of view (FoV) and complicate navigation and decision-making processes (*5*).

Moreover, urban settings involve a high density of vulnerable road users (VRUs), such as pedestrians and cyclists, whose behaviors are harder to predict compared to vehicular traffic. The presence of these VRUs, along with frequent and complex interactions at intersections, adds another layer of complexity to the operation of CAVs in urban environments. The chaotic nature of urban traffic, combined with the limited predictability of VRU movements, increases the likelihood of accidents, making urban scenarios a critical area of focus for further CAV research. (*2*) Occlusion, particularly, stands out as a major contributing factor to accidents in urban areas. It poses a significant impediment to the safety and efficiency of CAVs by blocking their sensors' FoV with static objects such as buildings and parked cars, as well as dynamic elements like other road users. Addressing the challenges posed by occlusion is essential for improving the safety and reliability of CAVs in urban contexts. (*4, 6*)

The concept of cooperative perception, facilitated by Vehicle-to-Everything (V2X) communication, has been proposed as concept of mitigating these issues (*4, 7, 8*). By enabling vehicles to share information about their surroundings with other CAVs (Vehicle-to-Vehicle, V2V) and the roadside infrastructure (Vehicle-to-Infrastructure, V2I), cooperative perception promises to enhance situational awareness and improve motion planning and decision-making of CAVs in urban areas. Furthermore, the use of CAVs and their detection and V2X capabilities has gained attention in the field of intelligent transportation systems research. In traffic engineering, this concept is commonly referred to as floating car observer (FCO) method and describes the use of extended floating car data (xFCD) for urban traffic safety and control applications. (*9–11*).

To address the previously mentioned challenges in CAV motion planning and decision-making and evaluate solutions such as cooperative perception and further applications such as the FCO method, robust simulation frameworks are required since real-world testing of CAVs in complex urban environments is still limited. Furthermore, simulation allows for the precise testing of various applications and a broad variety of scenarios. When it comes to the use and availability of simulation frameworks that take into consideration the previously described influencing factors of (cooperative) perception of CAVs, there is a lack of sophisticated open-source solutions that eliminate the need for complex co-simulation frameworks.

This paper is organized into five main sections. While the first one deals with the theoretical background, the second section introduces the methodology of the presented open-source

simulation framework. Afterwards, a case study for the evaluation of the simulation framework is introduced before the results of the case study are presented and discussed. Finally, a conclusion of this work is provided.

## LITERATURE REVIEW

The theoretical background for this study is presented in the following section. First, related work on FCO simulation studies and frameworks is discussed, before further elaborating on the consideration of occlusion effects in existing FCO studies. Finally, the contribution of this paper is presented.

### Related Work

Wardrop and Charlesworth (12) first proposed the Moving Observer (MO) method in the 1950s, which estimated traffic speed and traffic flow based on manual observations of surrounding traffic in both driving directions. With sensor technologies allowing vehicles nowadays to gather information about their surrounding, including xFCD with information about the ego vehicle and other road users, the originally proposed MO method is now commonly referred to as FCO method. For the evaluation of the FCO method, a variety of simulation studies with different methods, frameworks and applications of the FCO method have been conducted in the last years. The following Table 1 gives an overview of the related work.

When it comes to the observer vehicle considered in previous work, all studies have focused on vehicular traffic modes with private passenger cars being the predominating observer vehicle. Czogalla and Naumann (13) and Kühnel et al. (14) furthermore explored the potential of public transport vehicles as FCOs. Similarly, the detection of vehicular traffic modes has been considered in the majority of previous studies, while Gerner et al. (10) additionally considered the detection of VRUs (cyclists and pedestrians).

In regard to the simulation frameworks themselves, previous studies have proposed different solutions, each varying in complexity and functionalities depending on the application and the scope of the study. While microscopic traffic simulators provide information on each road user that can be used to further model the data-gathering process of a FCO, they are only capable of a 2D representation of the simulated scene. Co-simulation frameworks, on the other hand, offer a 3D representation of the simulated scene while introducing additional computational load and more effort in setting up the simulation (*10*). Furthermore, the use of commercial or open-source software tools differs between previous studies. While most co-simulation frameworks use SUMO as an open-source microscopic traffic simulation, CARLA is used as an open-source 3D simulation tool (*8, 18*). Pechinger et al. (19) presented hardware in the loop simulation framework with the microscopic traffic simulation AIMSUN, Simcenter Prescan as a 3D simulation tool, and a vehicle computer performing an AV's perception and motion planning. Frameworks utilizing microscopic traffic simulations without co-simulation also use SUMO as main open-source tool, while commercial software like VISSIM was used by Kühnel et al. (14) or AIMSUN used by Pechinger et al. (22).

Application-wise, the simulation frameworks have been proposed for different use cases. With the FCO method originally proposed by Wardrop and Charlesworth (12) for the assessment of traffic flows and speeds, it is often applied for traffic state estimation to obtain link-level traffic parameters (*9, 14, 16, 20*) and assess network-wide traffic states (*17, 21*). Object detection and classification is traditionally a computer vision problem, but at the same time a prerequisite for

**TABLE 1**: Literature overview of simulation studies on the floating car observer (FCO) method

| | | Source | Czogalla and Naumann (13) | Kühnel et al. (14) | Florin and Olariu (15) | Schäfer and Hoyer (*16*) | Van Erp et al. (17) | Langer et al. (9) | Li et al. (18) | Pechinger et al. (19) | Chen et al. (8) | Florin and Olariu (20) | Gerner et al. (10) | Zhang et al. (21) | Pechinger et al. (22) |
|---|---|---|---|---|---|---|---|---|---|---|---|---|---|---|---|
| | | Year | 2007 | 2009 | 2017 | 2017 | 2019 | 2020 | 2021 | 2021 | 2022 | 2023 | 2023 | 2023 | 2024 |
| Application | Visibility Analysis | | | | | | | | | | | | | | x |
| | Motion Planning | | | | | | | | | x | | | | | |
| | Object Detection and Classification | | | | | | | | x | x | x | | x | | |
| | Traffic State Estimation | x | x | x | x | x | x | x | | | | x | | x | |
| Simulation Framework | Code Published (open-source) | | | | | | | | | | | | x | x | x |
| | Open-Source | | | | | | | | x | | x | | x | x | |
| | Co-Simulation | | | | | | | | x | x | x | | | | |
| | Microscopic Traffic Simulation | x | x | x | x | x | x | x | | | | x | x | x | x |
| Observed Traffic Modes | Cyclists and Pedestrians | | | | | | | | | | | | x | | |
| | Passenger Cars | x | x | x | x | x | x | x | x | x | x | x | x | x | x |
| Observer Vehicle | Public Transportation | x | x | | | | | | | | | | | | |
| | Passenger Car | | x | x | x | x | x | x | x | x | x | x | x | x | x |

the real-world deployment of the FCO method for traffic efficiency and traffic safety applications. Therefore, simulation frameworks that generate a 3D representation of a FCO's surroundings, either as a camera image or a 3D point cloud, are often proposed for this task to eventually be used for more vehicle-related applications like motion planning (*8, 10, 18, 19*). Recently, Pechinger et al. (22) introduced a simulation framework for the visibility evaluation of urban intersections to investigate the occlusion effect of static and dynamic objects in a FCO vicinity and to evaluate the collective perception capabilities of CAV fleets in a broad and general manner.

**Occlusion Effects**

The occlusion of a FCO's FoV by sight-obstructing objects limits its ability to detect, classify, and track other road users and provide reliable xFCD for further applications. Different studies distinguish occlusion into static and dynamic occlusions. While static occlusion represents static objects, such as buildings, road signs, urban greenery (trees, bushes), and parked vehicles, dynamic occlusion represents temporary or moving objects such as cars, busses, trucks, bicycles, or pedestrians. (*11, 22–24*) In order to increase the validity of simulation studies that incorporate the FCO method, it is therefore important to account for these occlusion effects.

When it comes to the related work of this study, presented in Table 1, co-simulation frameworks allow for the consideration of occlusion effects due to their capability of representing a FCO's vicinity as a 3D scene, which can be used as input to object detection and classification algorithms (*8, 18, 19*). Microscopic traffic simulation frameworks, on the other hand, often only consider the effect of occlusions through simplistic assumptions (*14*) or do not consider it at all (*15, 17, 21*). Gerner et al. (10) consider occlusion effects in their simulation framework by creating an artificial 3D point cloud of a scene obtained from a microscopic traffic simulation and using the FCO's perspective of this scene as input for computer vision algorithms to detect other road users. Pechinger et al. (22), on the other hand, follows a ray tracing approach based on a microscopic traffic simulation to obtain a FCO's final FoV after considering static and dynamic occluding objects. The ray tracing approach generates rays from the center point of a FCO up to a distance of 30 meters, representing the non-occluded FoV of the FCO. If a ray intersects with a static or dynamic object, this intersection is used as the endpoint of the ray. Lastly, connecting the endpoints of all rays results in the final FoV of a FCO.

Furthermore, Gilroy et al. (7) shows that a FCO's detection rate depends on the level of occlusion, reflected in lower detection rates for objects that are visually more obstructed than others. They show that detection rates for partially and heavily occluded objects are substantially higher for the detection of passenger cars compared to that of VRUs (cyclists and pedestrians). This further highlights the necessity of incorporating VRUs in FCO simulation frameworks for the evaluation of urban traffic control and traffic safety applications.

**Own Contribution**

The simulation framework presented in this work is based on the previous work of Pechinger et al. (22) and has been adapted to address further identified needs and functions. Based on the literature review conducted for this study, requirements for the introduced simulation framework have been derived and considered during the development of the simulation framework. Four key requirements have been identified that reflect the contributions to the research field intended with this study:

As mentioned in the previous section, accounting for both static and dynamic occlusions in FCO simulation frameworks is crucial for ensuring the validity of study results. The ray tracing approach proposed by Pechinger et al. (22) has been recognized as an effective visualization method for the final FoV of a FCO, enhancing the clarity of the obtained results.

Furthermore, the proposed simulation framework emphasizes the consideration of VRUs in FCO simulations for evaluating urban traffic control and safety applications. By using a microscopic traffic simulation, the framework can model various road users, leveraging the capabilities of the utilized traffic simulation tool. Additionally, it introduces the observer vehicle type *Floating Bike Observer (FBO)* alongside the FCO. With the availability of sensor-equipped bicycles on the

market (*25*), the proposed simulation framework aims to facilitate simulation studies involving this new observer vehicle type.

Another advantage of the proposed simulation framework is that it eliminates the need for a co-simulation framework, thereby reducing the effort required for simulation configuration and decreasing the computational load.

Lastly, the proposed simulation framework relies entirely on open-source tools, utilizing SUMO for microscopic traffic simulation and a Python framework for subsequent steps. Additionally, the simulation framework is available on GitHub[1].

## SIMULATION FRAMEWORK

As described in the previous section, the proposed simulation framework builds upon the work of Pechinger et al. (22) and extends this to an open-source simulation framework with additional functionalities. While this study focuses on the application of the introduced simulation framework as originally proposed, further applications of the framework will be developed and incorporated into the framework in the future. The following sub-chapters elaborate on the different modules and functionalities of the framework, summarized in Figure 1.

### Input Data

The proposed simulation framework communicates with a microscopic traffic simulation through the use of SUMO and its interface TraCI (Traffic Control Interface) to retrieve the location of every static and dynamic road user for each time step of the simulation. Parked vehicles are considered static road users, while vehicular traffic, as well as VRUs (cyclists and pedestrians), are considered dynamic road users. Additionally, the simulation framework loads shapes and locations of static infrastructure elements from Open Street Map (OSM), such as buildings. Furthermore, shapes and locations of urban greenery, such as parks and trees, can be obtained from OSM.

If available, the framework can make use of a GeoJSON file containing information on the road space distribution of the considered scene. Used for visualization purposes only, it provides information on the locations and shapes of vehicular carriageways, parking areas, bicycle infrastructure as well as pedestrian sidewalks. The additional visualization of the road space has been shown to enable a faster understanding of the simulated scene.

The considered input data is often represented in different coordinate systems, which is why a transformation into a common coordinate reference system is performed to ensure the correct representation of all utilized geospatial data.

### Configuration Settings

The Python-enabled simulation framework offers users a wide range of functionalities that can be individually configured before initializing the framework. This enables a customized use of the offered functionalities, depending on the needs of individual users.

Within the *general settings*, users can activate the live visualization of the ray tracing which will animate the ray tracing performed by FCOs and FBOs. If the ray tracing visualization is activated, users can furthermore decide if the generated rays themselves or only the resulting visibility polygon of FCOs and FBOs should be visualized. Additionally, a manual forwarding option is integrated, which, when activated, requests a user's input to proceed to the calculation of the next

[1] https://github.com/TUM-VT/FTO-Sim

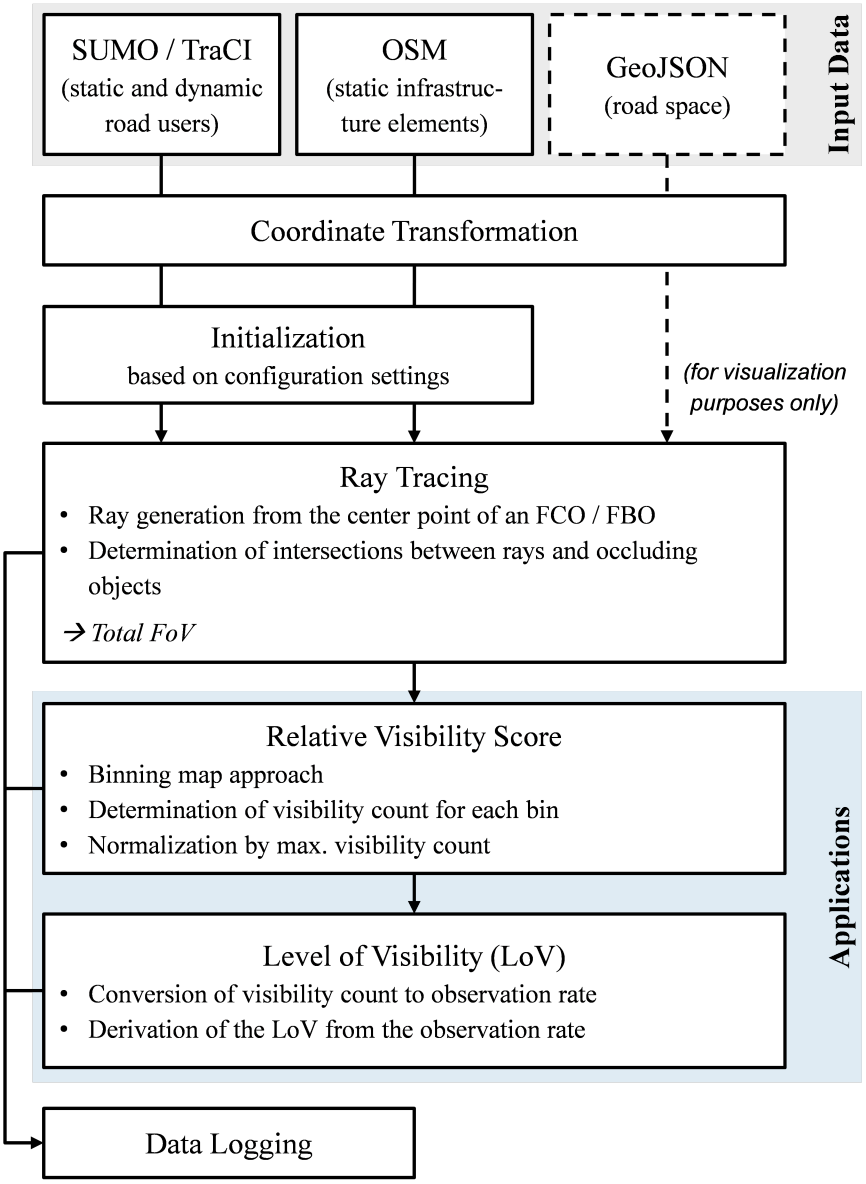


**FIGURE 1**: Methodological Overview of the Proposed Simulation Framework

frame. Furthermore, users can choose to save the animation after the simulation has been performed.

Through the *bounding box settings* users specify the extent of input data loading and the spatial boundaries of all further visualizations, enabling the simulation of scenarios with different spatial scopes.

The location of the SUMO simulation's configuration file and, optionally, a GeoJSON file for the visualization of the scenes road space to be utilized by the simulation framework are defined in the *path settings*.

The *warm-up settings* ensure an initial warm-up of the microscopic traffic simulation to allow for the generation of a reasonable traffic demand within the simulated traffic network before activating the ray tracing method.

The penetration rates of both FCOs and FBOs can be set individually within the *FCO / FBO settings*. Every generated vehicle and / or bicycle of the microscopic traffic simulation is assigned a random number of a uniform distribution ranging between [0,1] and if this number is below the defined FCO / FBO penetration rate, the vehicle or bicycle is assigned the vehicle type `'floating car observer'` or `'floating bike observer'`, respectively. Furthermore the number of rays that a FCO / FBO will generate during the ray tracing can be defined.

**Ray Tracing and Relative Visibility**

Based on the provided input data and configuration settings, the simulation framework is initiated and performs the ray tracing method for every FCO and FBO. In parallel to the ray tracing, a binning map approach is followed to update the visibility count of every bin that is included within the FoV of a FCO / FBO for every time step of the simulation. An overview of the working principle of the ray tracing method and the relative visibility analysis is given in Figure 2.

During the *initialization phase*, the simulation framework obtains the necessary input parameters from the loaded input data and configuration settings. Furthermore, a binning map is initialized that divides the simulated scene into equivalently sized squares and sets the visibility count of each bin to zero. The size of the bins and, with that, the resolution of the following visibility analyses (relative visibility and level of visibility) can be individually set by users of the simulation framework.

Once the *simulation loop* is initiated, the simulation framework will check the vehicle type of every vehicle and bicycle within the previously defined bounding box for each time step of the simulation. After the initially defined warm-up phase and depending on the defined FCO / FBO penetration rates, vehicles or bicycles with the vehicle type `'floating car observer'` or `'floating bike observer'` will be randomly generated and thus activating the ray tracing.

The *ray tracing module* will generate the previously defined number of rays descending from every observer's center point up to a distance of 30 meters. The angle between the rays will be equivalently sized to generate a non-occluded FoV in a circular form around an observer. Subsequently, the rays that intersect with static or dynamic objects are cut to obtain an observer's occluded FoV. Lastly, the endpoints of all rays are connected to create the visibility polygon representing the area within an observer's total FoV.

The *relative visibility* module updates the initialized binning map by increasing the visibility count of each cell within an observer's total FoV by one. In case of overlapping FoV's of multiple observers, the visibility count is still increased by one, thus following the methodology proposed by Pechinger et al. (22). The simulation loop is repeated until the simulation end is reached after which the final binning map and visibility counts are obtained. Additionally, the visibility counts are normalized by dividing each bin value by the maximum observed visibility count. Both resulting binning maps (raw visibility counts and LoV) are saved for further processing. Finally, a normalized visibility heat map is generated providing a visual representation of the spatiotemporal characteristics of the potential data collection process of FCOs / FBOs.

**Level of Visibility**

The Level of Visibility (LoV), as introduced by Pechinger et al. (22), provides a metric for comparing visibility across different scenarios under varying conditions. By converting the raw observation counts into an observation rate, defined as the frequency of observations of a bin over time, obtained from the observer's final FoVs, it provides a time-dependent scale for the comparison

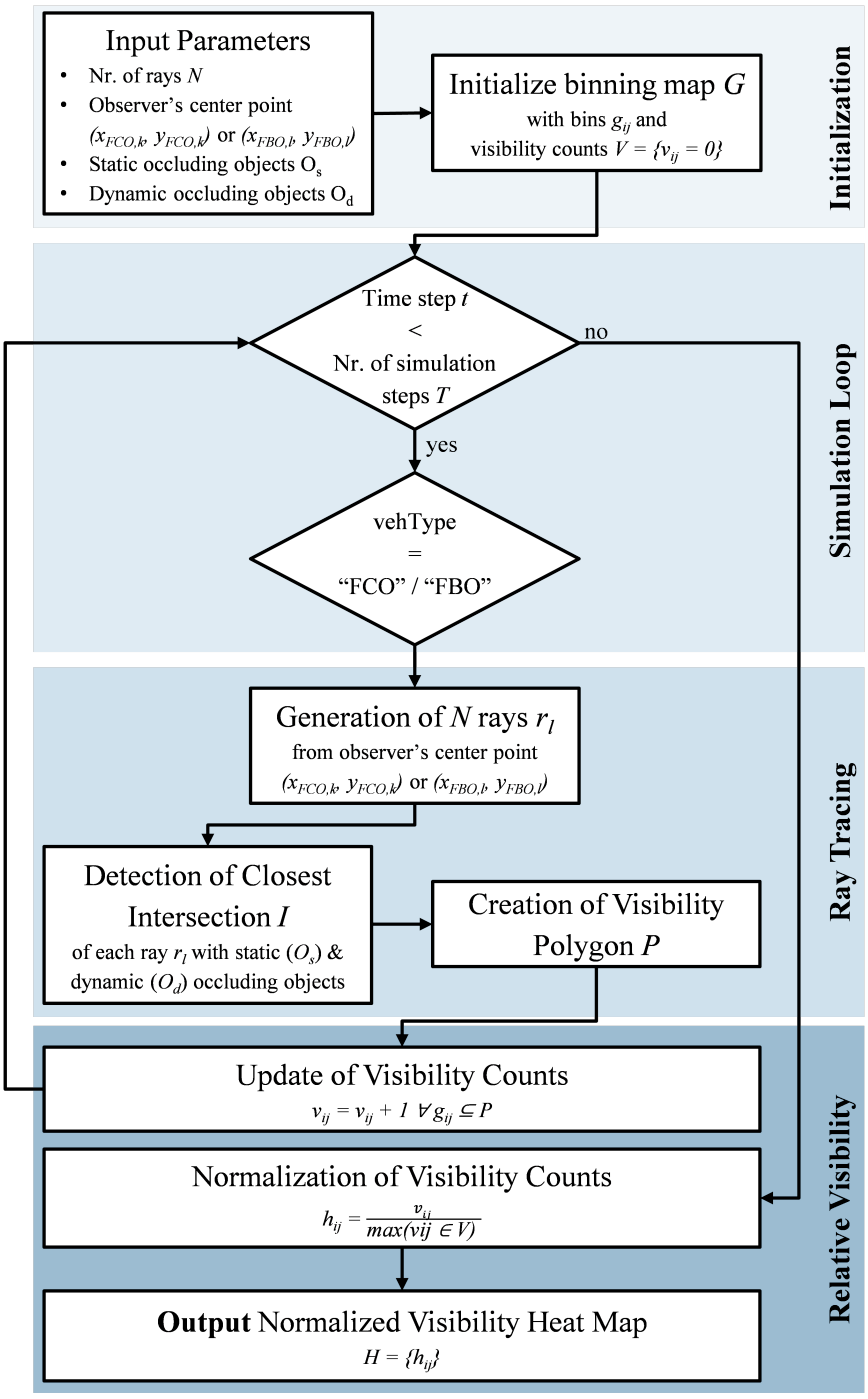


**FIGURE 2**: Working Principle of Ray Tracing and Relative Visibility

of different scenarios. Subsequently, the observation rate is categorized into one of five discrete LoVs offering a simplified representation of an observer's visibility conditions. Figure 3 gives an overview of the working principle of the LoV assessment.

Through the *initialization phase*, the LoV assessment is provided with the relevant input parameters and initializes arrays for both the LoV as well as the observation rate.

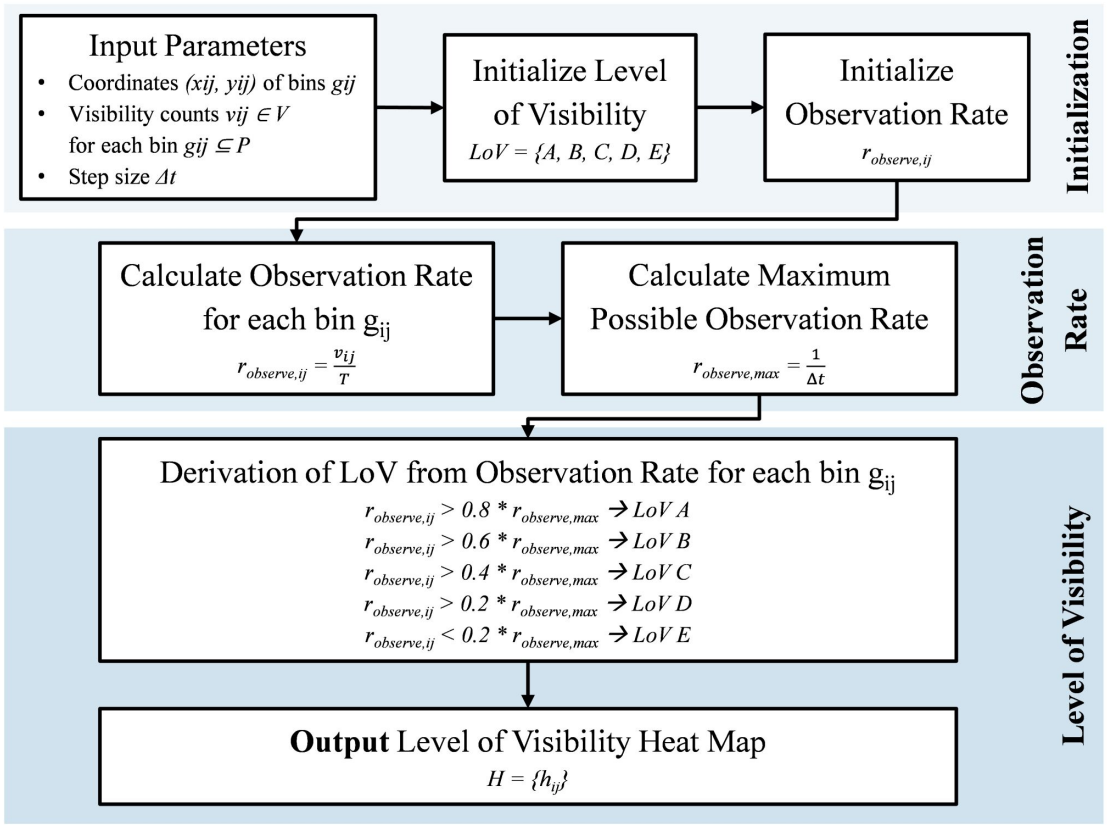


**FIGURE 3**: Working Principle of Level of Visibility Assessment

The *observation rate* is then calculated for each bin by dividing the visibility count by the simulation time. The maximum possible observation rate is defined in this study as the inverse of the simulation step size and, therefore, provides the possibility to account for differences in step sizes between different simulations.

Subsequently, the *level of visibility* for each bin is determined by assigning the observation rate to one of the five discrete LoVs, with the thresholds between different LoVs distributed equidistantly based on the maximum possible observation rate. Finally, a heat map of the simulated scene representing the assessed LoV for each bin is provided as a visual representation of the used metric.

## CASE STUDY

As suggested by Pechinger et al. (22) after proposing the LoV metric, further investigations are necessary for accurate calibration of the metric. On the one hand, the correlation between the LoV and the traffic volume is emphasized, since a larger number of observers navigating an area can obtain a greater number of observations. The authors anticipate that with increased demand, higher LoV categories may be attainable with lower penetration rates, whereas reduced demand might necessitate a considerably higher penetration rate. Furthermore, the LoV metric has only been investigated for non-signalized intersections so far. The substantial impact of traffic signalization on vehicle waiting times and queue formation is expected to have a significant influence on the LoV, making signalized intersections an interesting case for further calibration of the metric.

The goal of the case study of this work is to contribute to insights for the further calibration of the LoV metric, by considering additional traffic-related and infrastructural circumstances. To this end, the previously mentioned factors of varying traffic flows, as well as traffic signalization, have been considered. Additionally, the influence of one-way streets leading away from an intersection has been identified as an interesting use case for further calibrating the LoV metric.

**Intersection Layout**

The traffic network considered in the case study of this work is an urban signalized four-arm intersection located in the city center of Munich, Germany. Figure 4 shows a satellite image as well as the corresponding SUMO network utilized for this case study.

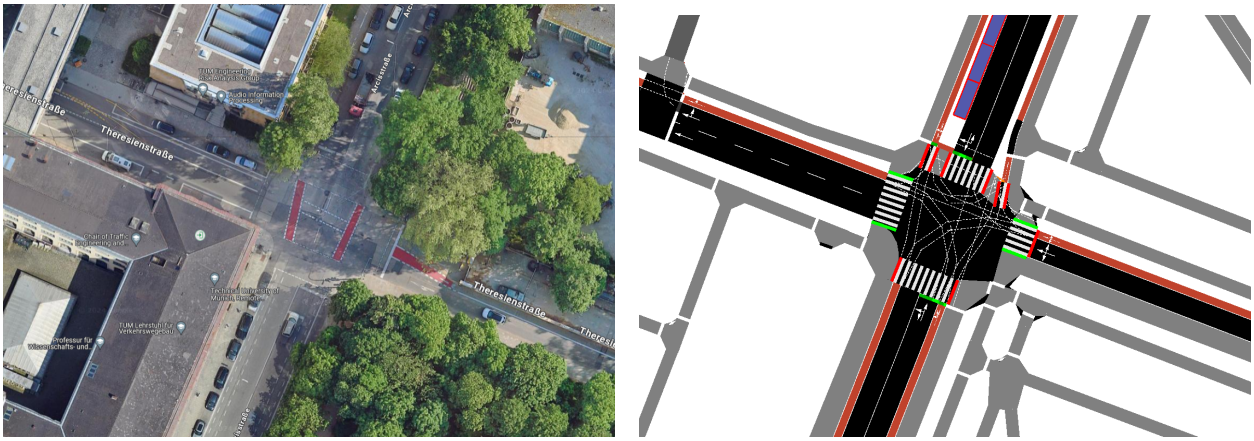


(a) Satellite Image (b) SUMO Network

**FIGURE 4**: Considered Intersection Layout

The considered urban intersection consists of a one-way street spanning from east to west, making the western intersection arm a one-way street leading away from the intersection. The northern and southern intersection arms feature one lane per driving direction. Bicycle lanes are available for all intersection arms and driving directions, while a row of parked vehicles is located between the vehicular carriageway and bicycle path in the northern approaching lane of the intersection. Further parking rows have been neglected for the SUMO network since they do not occlude the visibility between vehicular carriageways and bike paths as they are located between bike paths and pedestrian walkways. Pedestrians are not considered in this case study (see Figure 4b).

The considered traffic network, therefore, provides several infrastructural influences for the further calibration of the LoV metric: The investigation of a signalized intersection will reveal the impact of traffic signalization and its influence on vehicle waiting times and queue formations on the LoV metric. Considering a scenario with a one-way street allows for the investigation of a further element of urban intersection layouts, besides intersection arms providing lanes for both driving directions. Additionally, a one-way street leading away from the intersection (western intersection arm) provides further comparability for the evaluation of increased waiting times and queue formations at the remaining intersection arms by providing an intersection element where these effects do not occur.

**Traffic Demand**

The traffic demand considered for this case study has been partially obtained from loop detector data of the city of Munich. Peak hour traffic on an average weekday (Tue, June 4th 2024) has been considered for the vehicular traffic demand, while a generic bicycle demand has been assumed due to the lack of data. The following Table 2 shows the peak hour traffic demand for an average weekday for the considered intersection of this case study.

**TABLE 2**: Peak Hour Traffic Demand considered in this Case Study

| | | vehicle traffic demand | | | | bicycle traffic demand | | | |
|---|---|---|---|---|---|---|---|---|---|
| | | to | | | | to | | | |
| [veh/h] | | N | E | S | W | N | E | S | W |
| from | N | - | | 198 | 89 | - | | 70 | 40 |
| | E | 43 | - | 84 | 358 | 22 | - | 38 | 95 |
| | S | 56 | | - | 51 | 23 | | - | 25 |
| | W | | | | - | | | | - |

The traffic demand reflects a typical scenario for an urban intersection outside the main traffic network. The relatively low traffic volumes result in large time gaps between vehicles and no significant queue formation. Additionally, the inflow varies among the intersection arms, indicating a main inflow from the eastern intersection approach with about 480 veh/h. The northern and southern intersection approach provide a total intersection inflow of 290 veh/h and 105 veh/h, respectively.

The considered traffic demand, therefore, provides several traffic-related circumstances that allow for a more accurate calibration of the LoV metric. On the one hand, using real demand data allows for the application of the LoV metric to a realistic urban traffic scenario and provides a more profound basis for the calibration of the metric. On the other hand, the differences in the total intersection inflow of the different intersection arms provide a basis for the investigation of the correlation between the LoV and the traffic volume.

**Simulation Scenarios**

In order to obtain insights for the further calibration of the LoV metric, two different traffic demand scenarios are considered for this case study. Besides the previously described real traffic demand of the considered urban intersection, which is considered the *low demand scenario*, an additional *high demand scenario* is introduced to further investigate the performance of the LoV metric for extremely congested urban scenarios with signalized intersections. For the high-demand scenario, all traffic volumes are increased three-fold, leading to significantly lower time gaps between vehicles and the formation of extremely high queue lengths at the intersection.

Furthermore, the scenarios were performed with different *FCO penetration rates*, increasing incrementally by 10% from 10% to 100%.

For evaluating the case study, a *scenario run time* of 270 seconds has been chosen, including a 90-second warm-up phase, followed by a 180-second evaluation phase. For comparability to the obtained results of Pechinger et al. (22), the simulation time step has been set to 10 Hz and a number of 360 rays has been defined. The short simulation run time has been chosen in order to further evaluate the performance of the LoV metric in evaluating scenarios of different run times.

## RESULTS AND DISCUSSION

The following chapter presents the results of the case study. First, a visual representation of the ray tracing method is provided for both FCOs and FBOs. The results of the relative visibility and LoV evaluation are presented for examples of penetration rate scenarios illustrating the trends and patterns of the overall results. Based on those findings, proposals for the further calibration of the LoV metric will be discussed.

### Ray Tracing

A visualization for the ray tracing method is provided with the following Figure 5. The rays emerging from the center point of an observer are colored in blue when they are unobstructed and in red when they intersect with objects. The endpoints of all (unobstructed and intersected) rays are then connected to obtain the observer's visibility polygon, which represents the observer's final FoV.

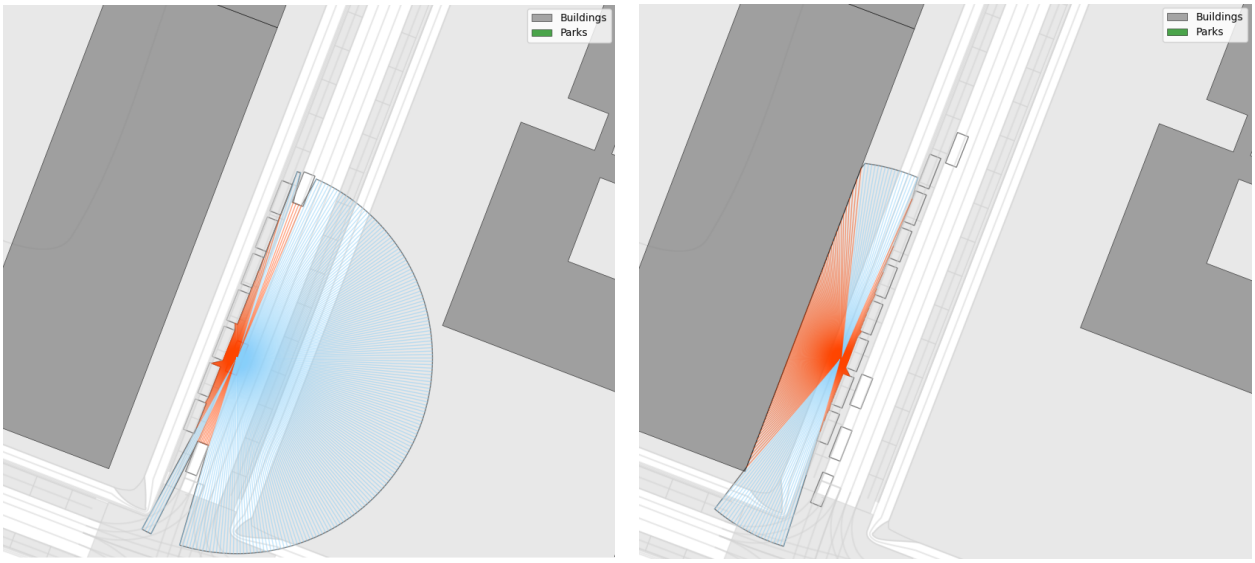


(a) Floating Car Observer (FCO) (b) Floating Bike Observer (FBO)

**FIGURE 5**: Ray Tracing Visualization (red rays intersect objects, blue rays are unobstructed)

The main difference between FCOs and FBOs is the different use of traffic infrastructure. While FCOs are bound to vehicular carriageways, FBOs are usually free to use both bicycle paths and vehicular carriageways in urban areas. The considered traffic network provides an insight into the difference between FCOs and FBOs with its northern intersection approach. While the row of parked vehicles blocks the FCO's view of the adjacent bicycle path, leading to occlusion effects and decreased visibility of the VRU infrastructure, the FBO is passing precisely this part of the VRU infrastructure. On the other hand, the row of parked vehicles is blocking the FBO's view of the adjacent vehicular carriageway.

Currently, the same FoV settings are considered for the different observer vehicles with an (unobstructed) ray length of 30 meters emerging from an observer's center point. Future work will include a more precise representation of both observer type's perception capabilities by adjusting the ray length depending on the observer type. By considering FBOs in the proposed simulation

framework, investigating a wide range of cooperative perception scenarios between different types of observer vehicles (in urban areas) is facilitated.

Figure 6 shows the case of multiple observations of the same area by different FCOs, represented by the overlapping visibility polygons of multiple observers. The borders of the visibility polygons are highlighted in green.

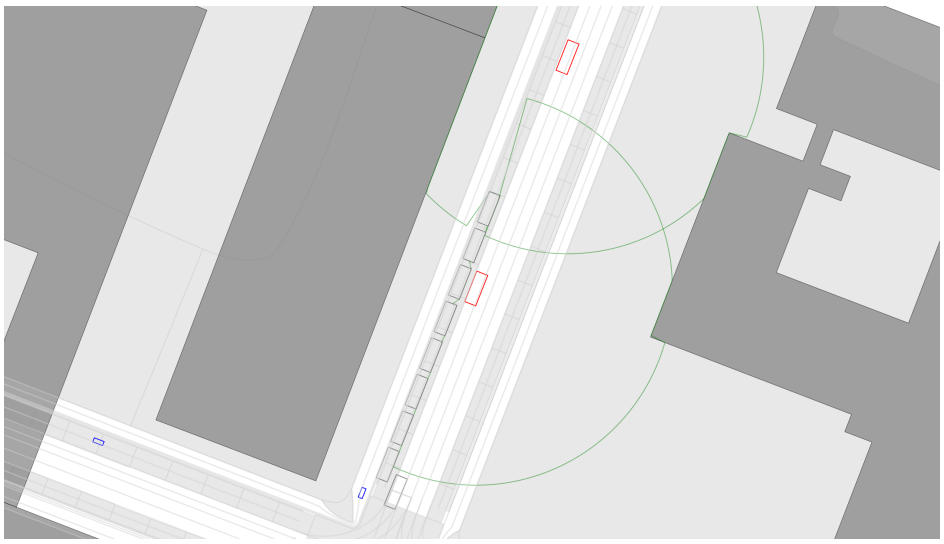

**FIGURE 6**: Overlapping Visibility Polygons of two FCOs

The LoV metric currently considers the visibility as a boolean-type variable with each bin being observed or unobserved during a simulation time step. This assumption seems valid regarding visibility assessment as the goal is to investigate occlusion effects in cooperative perception scenarios. Considering the observer's object classification capabilities, multiple simultaneous observations of the same area (ideally from different perspectives) add additional semantic value for the correct classification of road users, which should be considered for implementing future applications of the ray tracing method incorporated in the proposed simulation framework.

**Relative Visibility**

Heat maps representing the investigated scenario's relative visibility are created following the previously described ray tracing method. Relative visibility means that the obtained visibility counts are normalized by the maximum observed visibility count within the investigated scenario. This representation of results helps better understand the performance of the LoV metric and thus contributes to the further calibration of the metric. On the other hand, a comparison between different scenarios is not possible with the relative visibility assessment since every scenario yields different conditions for normalization. The following Figure 7 shows the relative visibility analysis for a single FCO as well as the high-demand scenario with a FCO penetration rate of 50 %.

The obtained results highlight the influence of traffic lights on the performance of the LoV metric. On the one hand, Figure 7a, including a single FCO crossing the intersection from north to west, highlights the influence of waiting times due to a signalized intersection. At very low velocities $v_{FCO} \sim 0\,\text{km/h}$, the area around the observer gets observed for a relatively long time period compared to areas that the observer passes with higher velocities. Furthermore, Figure 7b shows the relative visibility result for the investigated high-demand scenario with a FCO penetration rate

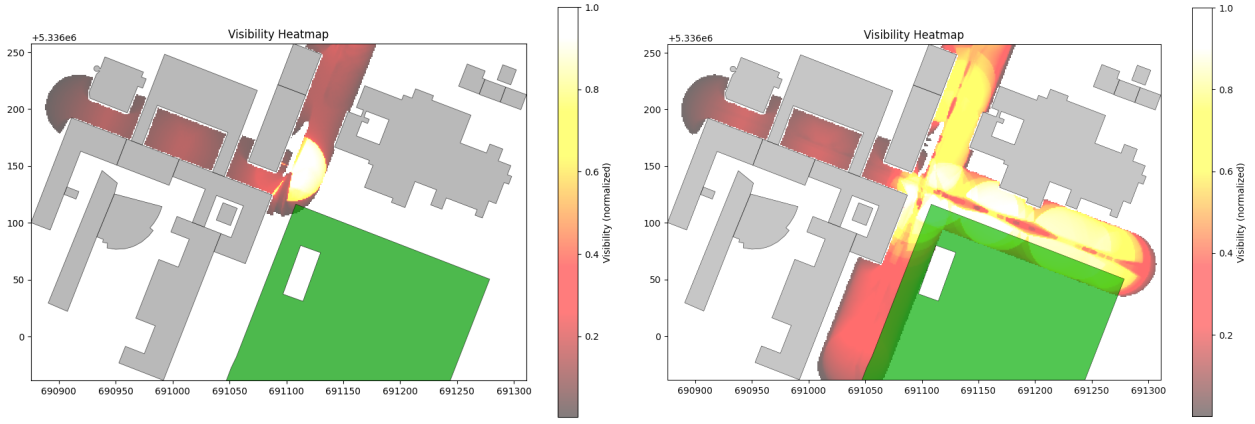


(a) high demand, single FCO

(b) high demand, 50% FCO penetration rate

**FIGURE 7**: Relative Visibility for different FCO configurations.

of 50 %. While the intersection approaches yield comparably high relative visibility scores, it can be observed that the visibility is significantly lower for the western intersection arm leading away from the intersection. This highlights the underestimation of visibility for one-way streets leading away from an intersection. While all intersection approaches experience observer velocities $v_{FCO} \sim 0\,\text{km/h}$ due to the previously described influence of traffic lights, no queues form at the western intersection arm during a red phase that would include observer vehicles with velocities $v_{FCO} \sim 0\,\text{km/h}$.

**Level of Visibility**

Figure 8 shows the obtained results for the LoV analysis. The figure highlights the difference between the low-demand and high-demand scenario exemplary for FCO penetration rates of 40 % and 90 %, respectively.

The obtained results highlight the correlation between traffic volumes and the LoV metric. The LoV heat maps show, that increased traffic volumes lead to substantially higher LoV scores for the same intersection layout. While a penetration rate of 90 % for the low-demand scenario leads to most of the inner intersection area resulting in a LoV B, a penetration rate of only 40 % for the high-demand scenario already leads to a LoV A for most of the inner intersection area. The extreme difference between the considered demand scenarios reveals a high sensitivity of the LoV metric towards changes in traffic volume. Additionally, the occlusion effect due to the parking row at the northern intersection approach can be observed.

Furthermore, the difference in total inflow from the different intersection approaches further reveals the correlation between traffic volumes and the LoV metric, which can be seen in particular in Figure 8d. While high queues form at the eastern intersection approach, leading to comparably low average velocities, a LoV A is obtained for most of the area. The northern and southern intersection approach, on the other hand, gain lower LoVs B and C, respectively, due to lower traffic volumes and higher average velocities.

A summary of observation rates for all considered demand scenarios and FCO penetration rates is provided in Figure 9. For both demand scenarios, the maximum and the mean observation rate have been obtained for the different penetration rates, before generating a sixth-grade

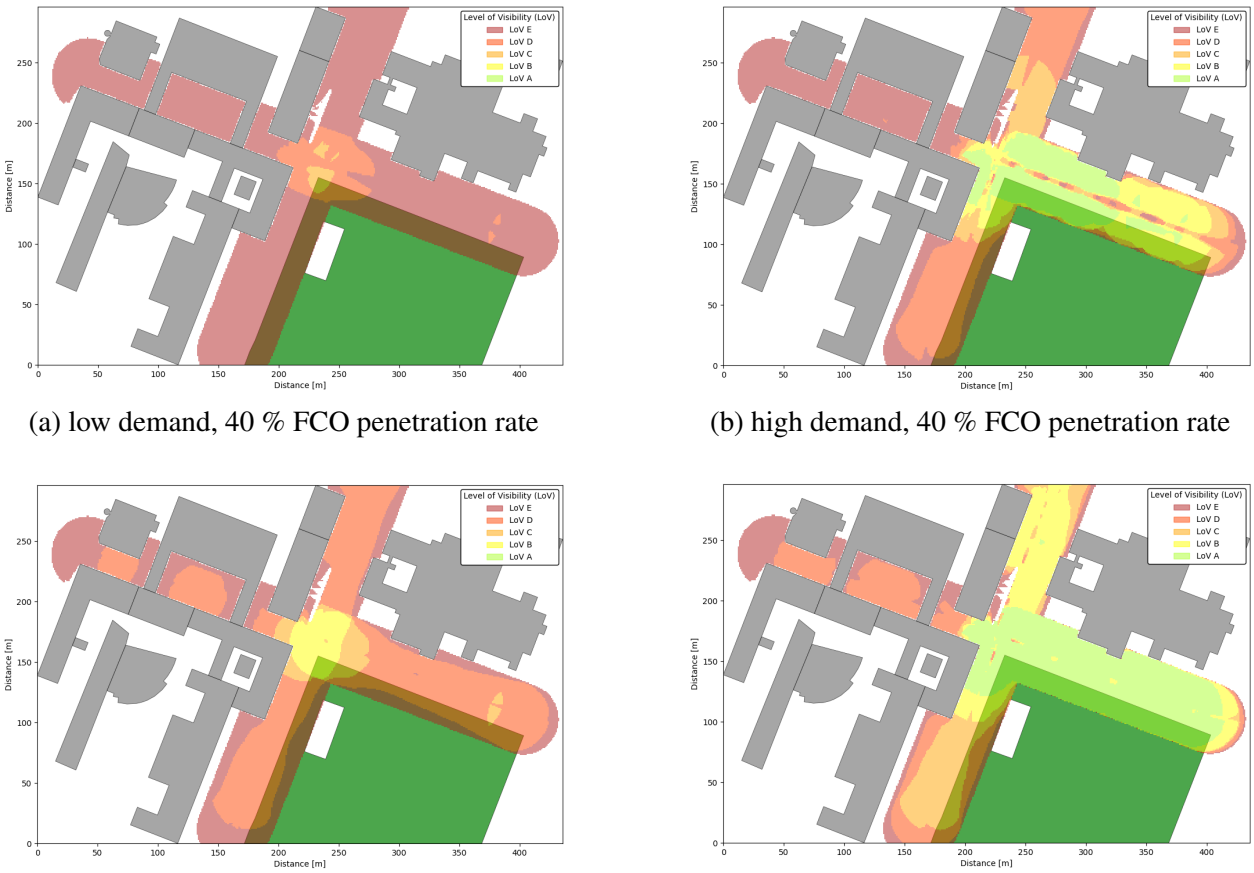


(a) low demand, 40 % FCO penetration rate

(b) high demand, 40 % FCO penetration rate

(c) low demand, 90 % FCO penetration rate

(d) high demand, 90 % FCO penetration rate

**FIGURE 8**: LoV Comparison for the considered Demand Scenarios

polynomial-fitted curve for each set of observations.

The results of the high-demand scenario show a rapid increase in the maximum observation rate, leading to maximum LoVs A for very low penetration rates of less than 10%. The maximum LoV curve saturates as expected at an observation rate of 10 observations per second. In contrast, the oscillation of the curve further signifies the rapid increase of maximum LoV observed for the high-demand scenario. With penetration rates of approximately 20%, an almost constant observation is achieved for single bins. On the other hand, the mean observation rate for the high-demand scenario shows a more steady increase with rising FCO penetration rates, resulting in a mean observation rate of approximately 6.5 observations per second for full penetration of FCOs.

For the low-demand scenario, significant differences compared to the high-demand scenario can be observed. While the maximum observation rate increases steadily with rising FCO penetration rates, a LoV of A can be obtained only for a full penetration of FCOs. The mean observation rate for the low-demand scenario generally remains on a comparably low level, increasing to a mean observation rate of approximately 3.0 observations per second for a full penetration of FCOs.

The difference in the observed demand scenarios reveals the strong correlation between traffic volumes and the LoV metric. While extremely high traffic volumes lead to overly congested scenarios and the frequent occurrence of the previously described effect of overestimating the vis-

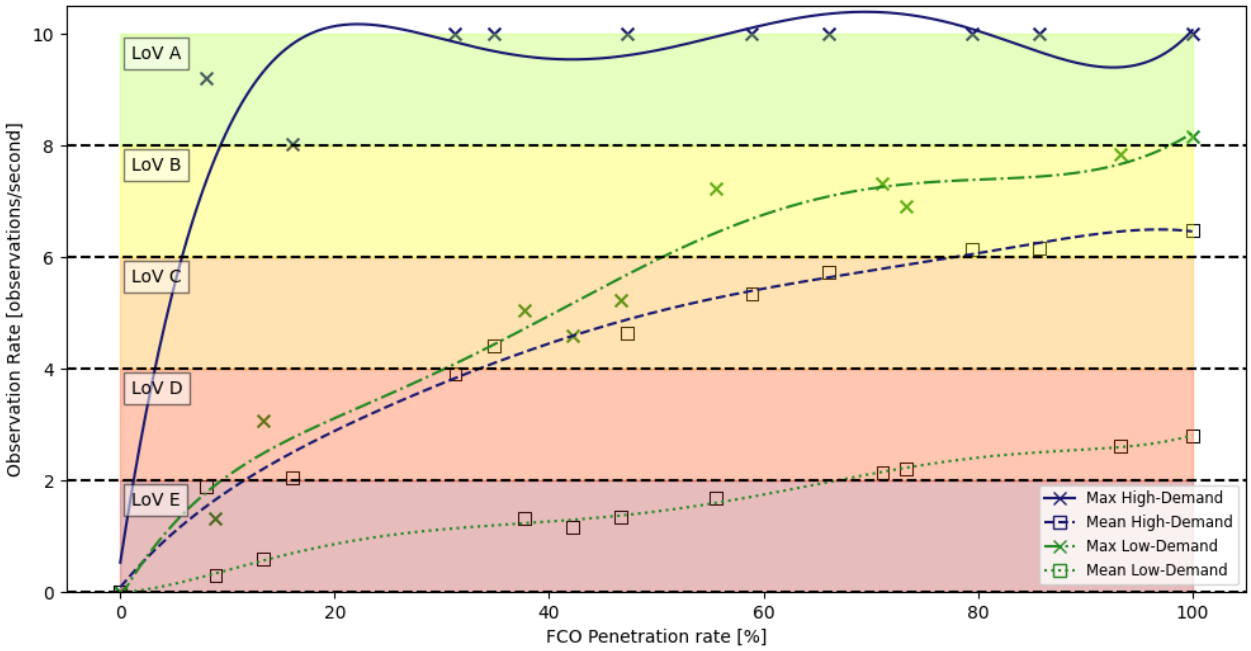


**FIGURE 9**: Summary of LoV results for the different considered scenarios

ibility for velocities $v_{FCO} \sim 0\,\text{km/h}$, low traffic volumes result in a significantly lower LoV. Since the low-demand scenario in this case study was obtained from real-work peak-hour traffic data, it appears that the LoV metric is unsuitable for real-world cases of signalized intersections with relatively low traffic volumes without further calibration. Contrary to that, the influence of observer velocities $v_{FCO} \sim 0\,\text{km/h}$ can lead to the metric assigning the best possible LoV A to scenarios with relatively low penetration rates, which is signalized by the curve for the maximum observation rate for the high-demand scenario. In comparison to Pechinger et al. (22), who found for a non-signalized intersection scenario the threshold of the maximum penetration rate to be at $\sim 34\%$ for reaching LoV A, the thresholds obtained for the discussed intersection layout and demand scenarios deviate significantly from this threshold. For the high-demand scenario, this threshold is $\sim 8\%$, whereas, for the low-demand scenario, the threshold moves to $\sim 98\%$. Especially considering that the low-demand scenario represents a real-life peak-hour demand scenario of an urban signalized intersection, the sensitivity of the LoV metric towards traffic volumes $q$ and observer velocities $v_{FCO}$ should be taken into consideration for the further calibration of the LoV metric.

**Proposals for Methodological Adaptions of the LoV Metric**

The main goal of the considered case study was to challenge the LoV metric to contribute to its further calibration and discuss proposals for methodological adaptions. The chosen intersection layout and demand scenarios have challenged the LoV metric as it is currently defined by investigating challenging scenarios giving new insights into the performance and sensitivity of the LoV metric.

Firstly, the obtained results highlight the correlation between the LoV metric and the traffic volume and the need for its further calibration. To overcome the LoV metric's extreme sensitivity to the traffic volume, the maximum possible observation rate and, with it, the LoV scale could be adjusted depending on the traffic volume. The maximum of the currently defined LoV scale is

represented as the constant observation of a bin, depending on the chosen simulation time step. In contrast, a demand-dependant adjustment of the LoV scale would inherently consider that it is not necessary to observe an area if no CAV is currently performing any actions in the considered area. Furthermore, the maximum of the LoV scale could be adjusted to represent the ideal frequency of observations that a CAV needs to perform its actions optimally, which would consider the technical needs of CAVs in the LoV assessment.

Furthermore, the investigation of a signalized intersection scenario has revealed the influence of observer velocities $v_{FCO} \sim 0\,\text{km/h}$ and with it, the systematical underestimation of visibility for one-way streets leading away from an intersection. This could be counteracted by considering an observer's velocity to assess the visibility score during the performed binning map approach. Instead of defining the visibility of each observed bin as a boolean variable, treating it as a float variable would enable the consideration of further influencing factors such as the observer's velocity or the distance between the observer and the observed bin. To evaluate this proposal for the methodological adaption of the LoV metric, further infrastructural factors have to be investigated.

Another factor that could be considered for the calibration of the LoV metric is the overlap of several visibility polygons. While an overlap does not influence a boolean type visibility count, the simultaneous detection of the same object by multiple observers can add semantic value to the detection of an object (e.g. for the classification of its type), which could be taken into account by treating the visibility count as a float variable.

## CONCLUSION

This paper introduces an open-source simulation framework incorporating methods for evaluating static and dynamic occlusion in urban environments. The framework is designed to model both FCOs and the newly introduced FBOs, reflecting the growing diversity of sensor-equipped vehicles in urban areas. The framework's SUMO and Python-based open-source architecture ensures the accessibility and adaptability for various applications. By not relying on complex co-simulation frameworks, but still considering complex occlusion effects, the framework ensures easier deployment and handling. First applications of the considered ray tracing method have been implemented, such as relative visibility assessment and the LoV metric, proposed by Pechinger et al. (22).

The performance and sensitivity of the LoV metric have been evaluated through a case study, contributing to further insights for its accurate calibration by highlighting its sensitivity to traffic volume and observer velocities. Potential methodological adaptions of the LoV metric have been discussed such as a demand-based adjustment of the LoV scale and the consideration of further influencing factors when assessing the visibility count. The discussed influencing factors include observer velocity, detection distances, and the simultaneous detection of objects by multiple observers.

Future work will include the further development and refinement of the introduced open-source simulation framework and the calibration of the LoV metric. Further applications of the ray tracing method, such as the provision of xFCD and use for traffic management applications or occlusion-aware motion planning for CAVs, will be developed and provided in the future. The calibration of the LoV metric will be achieved by investigating further infrastructural and demand-related sensitivities. Additionally, the framework will be extended to explore cooperative perception scenarios between FCOs and FBOs. While the ray tracing method has been implemented for FBOs already, the framework's applications do not consider it yet. Furthermore, other observer models besides the center point model will be integrated to better simulate real-world perception

capabilities.

**ACKNOWLEDGEMENTS**

This work is a result of the joint research project STADT:up. The project is supported by the German Federal Ministry for Economic Affairs and Climate Action (BMWK), based on a decision of the German Bundestag. The authors are solely responsible for the content of this publication.

The text in this work was refined using ChatGPT and Grammarly to improve readability. The referenced code in the Methodology section was written and debugged with the assistance of GitHub Co-Pilot, which improves code quality and reduces programming time.

The authors confirm contribution to the paper as follows: study conception and design: M. Ilic, M.Pechinger, E. Nexhipi; framework implementation: M. Ilic, M. Pechinger; analysis and interpretation of results: M. Ilic; draft manuscript preparation: M. Ilic, T. Niels, M. Pechinger, K. Bogenberger; All authors reviewed the results and approved the final version of the manuscript.

## REFERENCES


1. Tabone, W., J. de Winter, C. Ackermann, J. Bärgman, M. Baumann, S. Deb, C. Emmenegger, A. Habibovic, M. Hagenzieker, P. Hancock, R. Happee, J. Krems, J. D. Lee, M. Martens, N. Merat, D. Norman, T. B. Sheridan, and N. A. Stanton, Vulnerable road users and the coming wave of automated vehicles: Expert perspectives. *Transportation Research Interdisciplinary Perspectives*, Vol. 9, 2021, p. 100293.
2. Yigitcanlar, T., M. Wilson, and M. Kamruzzaman, Disruptive Impacts of Automated Driving Systems on the Built Environment and Land Use: An Urban Planner's Perspective. *Journal of Open Innovation: Technology, Market, and Complexity*, Vol. 5, No. 2, 2019.
3. Nastjuk, I., B. Herrenkind, M. Marrone, A. B. Brendel, and L. M. Kolbe, What drives the acceptance of autonomous driving? An investigation of acceptance factors from an end-user's perspective. *Technological Forecasting and Social Change*, Vol. 161, No. C, 2020.
4. Pechinger, M., G. Schröer, K. Bogenberger, and C. Markgraf, Roadside Infrastructure Support for Urban Automated Driving. *IEEE Transactions on Intelligent Transportation Systems*, Vol. 24, No. 10, 2023, pp. 10643–10652.
5. Yu, M.-Y., R. Vasudevan, and M. Johnson-Roberson, Occlusion-Aware Risk Assessment for Autonomous Driving in Urban Environments. *arXiv e-prints*, 2018, p. arXiv:1809.04629.
6. Staubach, M., *Identifikation menschlicher Einflüsse auf Verkehrsunfälle als Grundlage zur Beurteilung von Fahrerassistenzsystem-Potenzialen*. Phd thesis, Technical University of Dresden, 2010.
7. Gilroy, S., E. Jones, and M. Glavin, Overcoming Occlusion in the Automotive Environment—A Review. *IEEE Transactions on Intelligent Transportation Systems*, Vol. 22, No. 1, 2021, pp. 23–35.
8. Chen, H., B. Liu, X. Zhang, F. Qian, Z. M. Mao, and Y. Feng, *A Cooperative Perception Environment for Traffic Operations and Control*, 2022.
9. Langer, M., T. Schien, M. Harth, R. Kates, and K. Bogenberger, An Improved Moving Observer Method for Traffic Flow Estimation at Signalized Intersections. In *2020 IEEE Intelligent Vehicles Symposium (IV)*, 2020, pp. 1498–1503.
10. Gerner, J., D. Rößle, D. Cremers, K. Bogenberger, T. Schön, and S. Schmidtner, Enhancing Realistic Floating Car Observers in Microscopic Traffic Simulation. In *2023 IEEE 26th International Conference on Intelligent Transportation Systems (ITSC)*, 2023, pp. 2396–2403.
11. Zhang, C., F. Steinhauser, G. Hinz, and A. Knoll, Improved Occlusion Scenario Coverage with a POMDP-based Behavior Planner for Autonomous Urban Driving. In *2021 IEEE International Intelligent Transportation Systems Conference (ITSC)*, 2021, pp. 593–600.
12. Wardrop, J. G. and G. Charlesworth, A Method of Estimating Speed and Flow of Traffic from a Moving Vehicle. *Proceedings of the Institution of Civil Engineers*, Vol. 3, No. 1, 1954, pp. 158–171.
13. Czogalla, O. and S. Naumann, TRAVEL TIME ESTIMATION USING FLOATING CAR OBSERVERS, 2007.
14. Kühnel, C., C. Leitzke, and R. Hoyer, *Evaluation of Floating Car Observer Algorithms using microscopic Traffic Flow Simulation*, 2009.

15. Florin, R. and S. Olariu, On a Variant of the Mobile Observer Method. *IEEE Transactions on Intelligent Transportation Systems*, Vol. 18, No. 2, 2017, pp. 441–449.
16. *Verkehrszustandsschätzung mittels vernetzter Floating Car Observer*, 2017.
17. Van Erp, P. B., V. L. Knoop, and S. P. Hoogendoorn, On the value of relative flow data. *Transportation Research Procedia*, Vol. 38, 2019, pp. 180–200, journal of Transportation and Traffic Theory.
18. Li, P., A. Kusari, and D. J. LeBlanc, *A Novel Traffic Simulation Framework for Testing Autonomous Vehicles Using SUMO and CARLA*, 2021.
19. Pechinger, M., G. Schröer, K. Bogenberger, and C. Markgraf, Benefit of Smart Infrastructure on Urban Automated Driving - Using an AV Testing Framework. In *2021 IEEE Intelligent Vehicles Symposium (IV)*, 2021, pp. 1174–1179.
20. Florin, R. and S. Olariu, Real-Time Traffic Density Estimation: Putting on-Coming Traffic to Work. *IEEE Transactions on Intelligent Transportation Systems*, Vol. 24, No. 1, 2023, pp. 1374–1383.
21. Zhang, Y., M. Ilic, and K. Bogenberger, A Novel Concept of Traffic Data Collection and Utilization: Autonomous Vehicles as a Sensor. In *2023 IEEE 26th International Conference on Intelligent Transportation Systems (ITSC)*, 2023, pp. 3887–3892.
22. Pechinger, M., T. Niels, and K. Bogenberger, Threshold Analysis of Static and Dynamic Occlusion in Urban Areas: A Connected Automated Vehicle Perspective. *Transportation Research Record*, Vol. 0, No. 0, 2024, p. 03611981241230539.
23. Liu, Z., P. van Oosterom, J. Balado, A. Swart, and B. Beers, Detection and reconstruction of static vehicle-related ground occlusions in point clouds from mobile laser scanning. *Automation in Construction*, Vol. 141, 2022, p. 104461.
24. Kahn, M., A. Sarkar, and K. Czarnecki, I Know You Can't See Me: Dynamic Occlusion-Aware Safety Validation of Strategic Planners for Autonomous Vehicles Using Hypergames. *2022 International Conference on Robotics and Automation (ICRA)*, 2022, pp. 11202–11208.
25. Boréal Bikes, *Connected Micromobility – AI ADAS – V2X – AI-enabled sustainable mobility*, 2024, accessed: 2024-07-29.